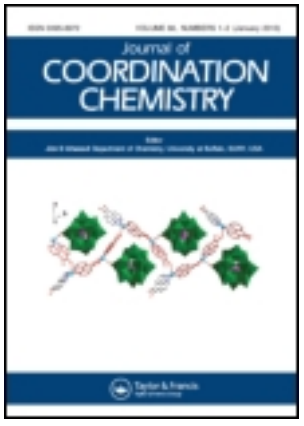

Journal of Coordination Chemistry
Publication details, including instructions for authors and subscription information:
http://www.tandfonline.com/loi/gcoo20

# Synthesis and characterization of dinuclear (Hedta)Ru(III) complexes with N-heterocyclic ligands: magnetic properties and DNA-binding studies

Jiangyun Wang[a], Xintong Zhao[b], Fang Yan[a], Liuya Wei[a], Qianxiu Pan[a], Fenglian Zhang[a] & Peipei Yang[c]

[a] Department of Medical Chemistry, Weifang Medical University, Weifang, P.R. China

[b] School of Medicine, Shandong University, Jinan, P.R. China

[c] College of Chemistry and Materials Science, Huaibei Normal University, Huaibei, P.R. China

Accepted author version posted online: 25 Sep 2013.Published online: 15 Nov 2013.

To cite this article: Jiangyun Wang, Xintong Zhao, Fang Yan, Liuya Wei, Qianxiu Pan, Fenglian Zhang & Peipei Yang (2013) Synthesis and characterization of dinuclear (Hedta)Ru(III) complexes with N-heterocyclic ligands: magnetic properties and DNA-binding studies, Journal of Coordination Chemistry, 66:21, 3848-3856, DOI: 10.1080/00958972.2013.848274

To link to this article: http://dx.doi.org/10.1080/00958972.2013.848274

*Journal of Coordination Chemistry*, 2013
Vol. 66, No. 21, 3848–3856, http://dx.doi.org/10.1080/00958972.2013.848274



# Synthesis and characterization of dinuclear (Hedta)Ru(III) complexes with N-heterocyclic ligands: magnetic properties and DNA-binding studies

JIANGYUN WANG†, XINTONG ZHAO‡[1], FANG YAN†, LIUYA WEI†, QIANXIU PAN†, FENGLIAN ZHANG† and PEIPEI YANG*§

†Department of Medical Chemistry, Weifang Medical University, Weifang, P.R. China
‡School of Medicine, Shandong University, Jinan, P.R. China
§College of Chemistry and Materials Science, Huaibei Normal University, Huaibei, P.R. China

(*Received 25 January 2013; accepted 4 September 2013*)

Two ruthenium(III) complexes containing ethylenediaminetetraacetate(edta), viz. $[\{Ru(Hedta)\}_2L]\cdot xH_2O$ L = 4,4′-bipyridine(bpy) (**1**) and 4,4′-azopyridine(Azpy) (**2**), have been synthesized by the reaction between $K[Ru(Hedta)Cl]\cdot 1.5H_2O$ and the corresponding N-heterocycles. Complex **1** was determined by single-crystal X-ray diffraction. The products were characterized by IR, UV–vis, cyclic voltammetry, and magnetic techniques. Their DNA-binding activities were investigated using electronic absorption spectroscopic methods and fluorescence quenching; the experimental results show that these two ruthenium complexes may bind to CT-DNA through intercalation modes.

*Keywords*: (Hedta)Ru(III) Complexes; N-Heterocycles; Magnetic properties



## 1. Introduction

Self-assembly of functional supramolecular complexes has attracted considerable attention. N-Heterocyclic ligands, such as 4,4′-bipyridine(bpy) and 4,4′-azopyridine(Azpy), are of general interest because of their ability to construct supramolecular architectures with covalent interactions and noncovalent interactions (hydrogen bonds, $\pi$–$\pi$ stacking interactions, etc.) [1, 2]. There is also considerable current interest in the chemistry of ruthenium–EDTA complexes, known for fascinating redox, photophysical, and other various properties, especially their favorable biological activity, such as DNA-binding and DNA photocleavage properties [3, 4].

Many studies suggest that ruthenium complexes are ideal templates of DNA-interactive systems, which can be designed as potential anticancer drugs for effective, less toxic, and target-specific properties [5]. Compared with Ru(II) complexes, DNA-binding studies for Ru(III) complexes, especially Ru(III)–EDTA complexes, are infrequently reported [6–8].

*Corresponding author. Email: hbnuypp@163.com
[1]Co-first author

These types of complexes can bind to DNA in many ways, such as electrostatic interactions, intercalation, groove binding, etc.

In this article, we use Ru(Hedta) as a building block for construction of polymeric structures with 4,4′-bipyridine and 4,4′-azopyridine. We report herein the synthesis and other properties of $[\{Ru(Hedta)\}_2(bpy)]\cdot 2H_2O$ (**1**) and $[\{Ru(Hedta)\}_2(Azpy)]\cdot 12H_2O$ (**2**), and we also investigate the X-ray structure of **1**.

## 2. Experimental

### 2.1. *Materials and methods*

$K[Ru(Hedta)Cl]\cdot 1.5H_2O$ was prepared as described [9]. 4,4′-Bipyridine and 4,4′-azopyridine were of reagent grade and used without purification. C, H, and N elemental analyzes were carried out with a Perkin-Elmer analyzer, model 240. Electronic spectra were recorded with a Shimadzu UV-2101PC spectrophotometer from 200 to 2000 nm at room temperature. The FT-IR spectra were recorded with KBr pellets from 4000 to 400 $cm^{-1}$ with a Bio-Rad FTS 135 spectrometer.

### 2.2. *Synthesis of $[\{Ru(Hedta)\}_2(bpy)]\cdot 2H_2O$ (1)*

A solution of $K[Ru(Hedta)Cl]\cdot 1.5H_2O$ (98 mg, 0.2 mM) was slowly added to one arm of an H-shaped tube and a solution of bpy (20 mg, 0.1 mM) in acetone was slowly added to the other arm. After slow diffusion for four weeks, orange single-crystals suitable for X-ray diffraction were obtained. Elemental analysis (%) for $C_{30}H_{38}N_6O_{18}Ru_2$ (Fw. 972.80): Anal. Calcd: C, 37.01; H, 3.91; N, 8.63. Found: C, 37.18; H, 3.82; N, 8.66. IR spectrum in KBr, selected bands, $cm^{-1}$, 3426 s, ν(O–H); 1651 s, ν(C=O); 1290 m, $\nu_s$(C=O).

### 2.3. *Synthesis of $[\{Ru(Hedta)\}_2(Azpy)]\cdot H_2O$ (2)*

Complex **2** was prepared using a similar method to **1** using Azpy instead of bpy. Orange microcrystals were obtained in three weeks by slow diffusion. Unfortunately, single crystals for this complex suitable for X-ray diffraction were not obtained although we tried many techniques. Elemental analysis (%) for $C_{30}H_{36}N_8O_{17}Ru_2$ (Fw. 982.80): Anal. Calcd: C, 36.63; H, 3.66; N, 11.40. Found: C, 36.51; H, 3.64; N, 11.49. IR spectrum in KBr, selected bands, $cm^{-1}$, 3424 s, ν(O–H); 1651 s, $\nu_{as}$(C=O); 1290 m, $\nu_s$(C=O).

### 2.4. *X-ray crystallographic study*

All measurements were made on a Bruker SMART diffractometer equipped with a graphite monochromator and Mo Kα radiation ($\lambda$ = 0.71073 Å). The structure was solved by direct methods and refined by full-matrix least-squares. Hydrogens were added geometrically and refined by mixed method. All calculations were performed using SHELEX-97.

## 3. Results and discussion

### 3.1. *Synthesis and general characterization*

Crystallographic data and processing parameters for structural analyzes of **1** are summarized in table 1. The coordination environment of **1** is shown in figure 1, selected bond lengths and angles are listed in table 2.

As shown in figure 1, each Ru(Hedta) is connected by 4,4′-bpy, and Ru(III) is six-coordinate to give a slightly distorted octahedron similar to $[\{Ru(Hedta)\}_2(Pyz)]\cdot 8H_2O$ we reported previously [10]. The Ru–O(carboxylate) bond lengths, Ru(1)–O(1), Ru(1)–O(3), and Ru(1)–O(7), are of 1.987(4), 2.008(4), and 1.993(4) Å, similar to those for *trans* carboxylate in (Hedta)Ru(III) complexes reported. The Ru–N bond distances range from 2.043 (4) to 2.128(5) Å, in the normal range of Ru–N bonds. The distance between Ru(1) and Ru(1A) is 7.231 Å. The bond angles around Ru(III) range from 83.67(19) to 95.77(16), close to octahedral. Extensive hydrogen bonds are formed through interactions of the carboxylic group, methylene, and water, which made the whole system into a 3-D structure (figure 2).

### 3.2. *IR spectra*

The IR spectra for **1** and **2** are very similar. The broad adsorption at 3420–3430 $cm^{-1}$ characterizes the overlapping peak of OH of water and carboxylic groups. The peaks at 1651 $cm^{-1}$ for **1** and 1652 $cm^{-1}$ for **2** could be assigned to the asymmetric stretch of carboxylate ($\nu_{as}(COO^-)$), and the peaks at 1295 $cm^{-1}$ for **1** and 1290 $cm^{-1}$ for **2** could be assigned to the symmetric stretch of carboxylate ($\nu_s(COO^-)$); the value of $\Delta\nu_{as-s} > 200$ $cm^{-1}$ reveals the presence of monodentate carboxylate [11, 12], consistent with X-ray diffraction analysis.

Table 1. Crystal and refinement data for **1**.

| | |
|---|---|
| Empirical formula | $C_{30}H_{38}N_6O_{18}Ru_2$ |
| Formula weight | 972.80 |
| Temperature [K] | 293(2) |
| Wavelength [Å] | 0.71073 |
| Crystal system | Monoclinic |
| Space group | *P2(1)/c* |
| *a* [Å] | 7.2610(7) |
| *b* [Å] | 13.2987(14) |
| *c* [Å] | 18.4627(19) |
| *α* [°] | 90 |
| *β* [°] | 91.219(2) |
| γ [°] | 90 |
| *V* [Å$^3$], *Z* | 1782.4(3), 2 |
| $D_{Calcd}$ [Mg $m^{-3}$] | 0.813 |
| *μ* [$mm^{-1}$] | 0.937 |
| *F* (000) | 984 |
| Crystal size [mm] | 0.22 × 0.16 × 0.12 |
| Goodness-of-fit on $F^2$ | 1.038 |
| Limiting indices | $-8 \le h \le 8$, $-15 \le k \le 15$, $-21 \le l \le 14$ |
| *R*1, *wR*2 [$I > 2\sigma(I)$] | *R*1 = 0.0437, *wR*2 = 0.1079 |
| *R*1, *wR*2 (all data) | *R*1 = 0.0633, *wR*2 = 0.1188 |

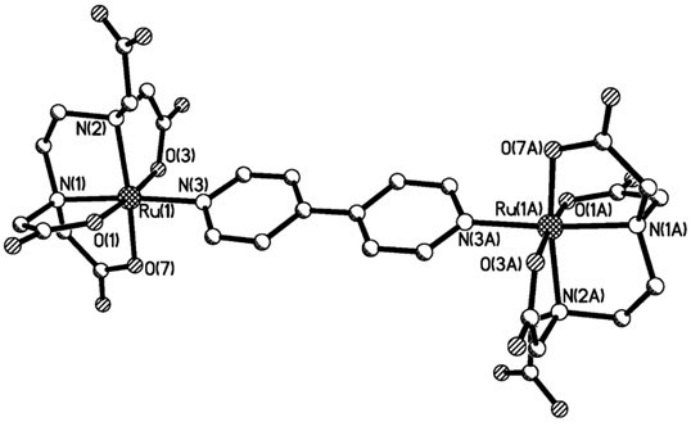


Figure 1. Molecular structure of **1** (hydrogens omitted for clarity).

Table 2. Selected bond lengths [Å] and angles [°] for **1**.

| | | | |
|---|---|---|---|
| Ru(1)–O(1) | 1.987(4) | Ru(1)–N(1) | 2.043(4) |
| Ru(1)–O(3) | 2.008(4) | Ru(1)–N(2) | 2.128(5) |
| Ru(1)–O(7) | 1.993(4) | Ru(1)–N(3) | 2.079(4) |
| O(1)–Ru(1)–O(7) | 95.77(16) | O(7)–Ru(1)–O(3) | 88.55(18) |
| O(1)–Ru(1)–O(3) | 174.93(17) | O(1)–Ru(1)–N(1) | 84.23(17) |
| O(7)–Ru(1)–N(1) | 83.67(19) | O(3)–Ru(1)–N(1) | 93.64(17) |
| O(1)–Ru(1)–N(3) | 92.52(16) | O(7)–Ru(1)–N(3) | 92.81(17) |
| O(3)–Ru(1)–N(3) | 89.91(16) | N(1)–Ru(1)–N(3) | 174.94(18) |
| O(7)–Ru(1)–N(2) | 166.4(2) | O(1)–Ru(1)–N(2) | 93.54(17) |
| O(3)–Ru(1)–N(2) | 81.75(19) | N(1)–Ru(1)–N(2) | 87.4(2) |
| N(3)–Ru(1)–N(2) | 96.72(19) | | |

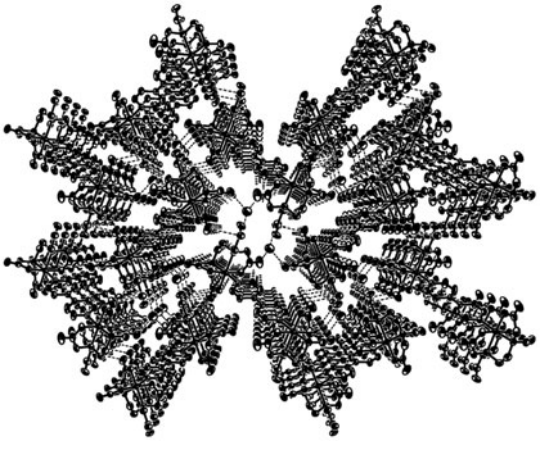

Figure 2. View of the 3-D structure of **1**.

### 3.3. *UV–vis spectra*

The UV–vis spectra of **1** and **2** in DMSO were measured at room temperature and are very similar to the Ru(Hedta) complexes reported [10, 13]. The electronic spectrum of **1** shows two intense absorptions at 258 nm ($\varepsilon$ = 9777 $M^{-1}\,cm^{-1}$) and 318 nm ($\varepsilon$ = 2733 $M^{-1}\,cm^{-1}$), similar to that of **2** with two bands at 258 nm ($\varepsilon$ = 9882 $M^{-1}\,cm^{-1}$) and 286 nm ($\varepsilon$ = 7294 $M^{-1}\,cm^{-1}$). These are assigned to ligand-to-metal charge-transfer transitions (LMCT). The other two relatively weak absorptions in the visible region, 736 nm ($\varepsilon$ = 45.8 $M^{-1}\,cm^{-1}$) for **1** and 735 nm ($\varepsilon$ = 27.7 $M^{-1}\,cm^{-1}$) for **2**, are assigned to the *d–d* transition $^2T_{2g} \rightarrow {}^2A_{2g}$.

### 3.4. *Cyclic voltammetric studies*

The cyclic voltammograms (figure 3) of **1** and **2** in DMSO were carried out at a platinum disk working electrode using [$Bu_4$ N][$ClO_4$](TBAP) as the supporting electrolyte with a scan rate of 100 mV/s; the results (*versus* $FcH/FcH^+$) are given in table 3. Successive metal-based couples for **1**, $Ru^{III}$–$Ru^{III}$ → $Ru^{III}$–$Ru^{IV}$ and $Ru^{III}$–$Ru^{IV}$ → $Ru^{IV}$–$Ru^{IV}$, appear at 288 and 697 mV. In addition, two reversible reductions at −238 and −657 mV correspond to one-electron reduction of $Ru^{III}$–$Ru^{III}$ ⇋ $Ru^{III}$–$Ru^{II}$ ($E_{pc}$ = −333 mV, $E_{pa}$ = −238 mV) and $Ru^{III}$–$Ru^{II}$ ⇋ $Ru^{II}$–$Ru^{II}$ ($E_{pc}$ = −741 mV, $E_{pa}$ = −657 mV); both of the reduction processes are reversible with peak-to-peak separation ($\Delta E$p) values of 95 and 84 mV, respectively, and $I_{pa}/I_{pc} \approx 1$, which are characteristic of a single-step, one-electron transfer [14, 15]. Another irreversible reduction at $E_{pc}$ = −1138 mV may be assigned as the bpy-based reduction. Compared with **1**, there is only one irreversible oxidation at 676 mV, and no other bands appear at 300 mV in the range of 0–1.5 V, indicating the oxidation of both ruthenium(III) centers occurs at the same potential, corresponding to $Ru^{III}$–$Ru^{III}$ → $Ru^{IV}$–$Ru^{IV}$. The same oxidated electric potential between two $Ru^{III}$ centers indicates electronic interactions reduce with the increasing length of the bridging ligand [16]. One reversible reduction at −295 mV corresponds to one-electron reduction of $Ru^{III}$–$Ru^{III}$ ⇋ $Ru^{III}$–$Ru^{II}$ ($E_{pc}$ = −406 mV, $E_{pa}$ = −295 mV, $\Delta E_p$ = 111 mV, $I_{pa}/I_{pc}$ = 1.5), similar to **1**, and another irreversible reduction at −711 mV corresponds to $Ru^{III}$–$Ru^{II}$ → $Ru^{II}$–$Ru^{II}$. Another quasi-reversible reduction at $E_{pc}$ = −1064 mV may be assigned as Azpy-based reduction.

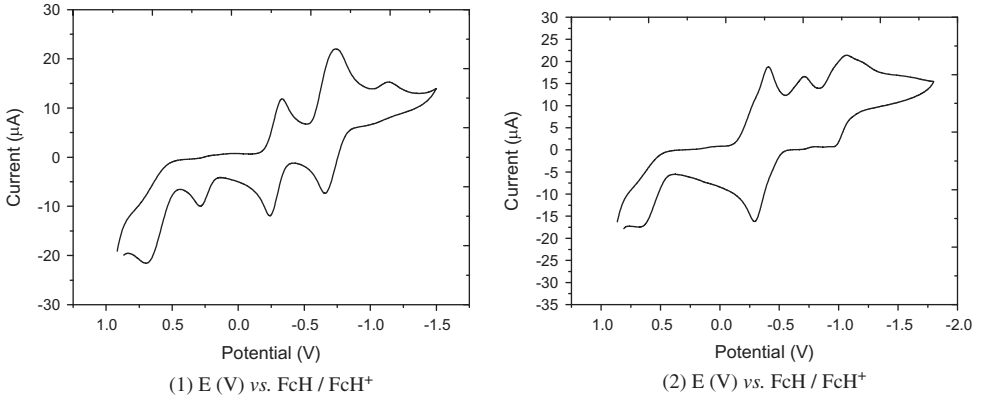


Figure 3. CV diagram of **1** and **2**.

Table 3. Cyclic voltammetric data for **1** and **2**.

| Complex | Couple | $I_{pa}/I_{pc}$ | $E_{pa}$/mV ($\Delta E_p$/mV) | $E_{pc}$ (mV) | $E_{1/2}$ (mV) |
|---|---|---|---|---|---|
| **1** | $Ru^{III}$–$Ru^{III} \rightarrow Ru^{III}$–$Ru^{IV}$ | – | 288 | – | – |
| | $Ru^{III}$–$Ru^{IV} \rightarrow Ru^{IV}$–$Ru^{IV}$ | – | 676 | – | – |
| | $Ru^{III}$–$Ru^{III} \leftrightharpoons Ru^{III}$–$Ru^{II}$ | 1.0 | −238(75) | −333 | −285.5 |
| | $Ru^{III}$–$Ru^{II} \leftrightharpoons Ru^{II}$–$Ru^{II}$ | 1.2 | −657(84) | −741 | −699 |
| | bpy reduction | – | – | −1138 | – |
| **2** | $Ru^{III}$–$Ru^{III} \rightarrow Ru^{IV}$–$Ru^{IV}$ | – | 676 | – | – |
| | $Ru^{III}$–$Ru^{III} \leftrightharpoons Ru^{III}$–$Ru^{II}$ | 1.5 | −295(111) | −406 | −350.5 |
| | $Ru^{III}$–$Ru^{II} \rightarrow Ru^{II}$–$Ru^{II}$ | – | – | −711 | – |
| | Azpy reduction | 1.6 | −950(113) | −1063 | −1006.5 |

The difference between the cyclic voltammetric studies for **1** and **2** implies that the electronic interactions between ruthenium centers are affected by the length of the bridging ligand [17].

### 3.5. *Magnetic properties*

Complex **1** exhibited a magnetic moment of 2.66 B.M. at 300 K, slightly higher than that expected for a binuclear low-spin ruthenium system. As shown in figure 4, upon cooling, the $\mu_{eff}$ curve for **1** continuously increases to a maximum (2.83 B.M.) at 6.5 K. This behavior of the $\mu_{eff}$ curve shows ferromagnetic interactions in **1**. However, the curve drops abruptly below 6.5 K, indicating that an antiferromagnetic interaction exists at lower temperatures.

The pronounced decrease of the magnetic moment with temperature suggests a ferromagnetic interaction between neighboring ruthenium(III) ions; the model used to fit the magnetic data considers a general isotropic exchange spin Hamiltonian $H = -2\,JS_1S_2$ ($S_1 = S_2 = 1/2$), using the Bleaney–Bowers equation (1) [18, 19], which also considers molecular field approximation and a weak intermolecular antiferromagnetism. We can fit our experimental data with the total equation (2):

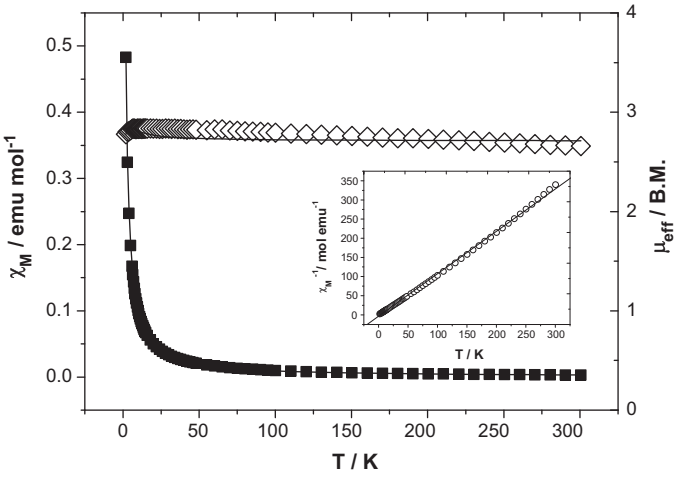


Figure 4. $\chi_M$(■) *vs.* *T* and $\mu_{eff}$(□) *vs.* *T* plots for **1**. The inset is the $1/\chi_M$(○) *vs.* *T* for **1**.

$$\chi_M = \frac{2Ng^2\beta^2}{3kT}\frac{1}{1+\frac{1}{3}\exp(-2J/kT)} \quad (1)$$

$$\chi_{tatal} = \chi_M/[1-\chi_M(zJ'/Ng^2\beta^2)] \quad (2)$$

Leading to the following values: $J$ = 2.0 cm$^{-1}$, $zJ'$ = −0.5 cm$^{-1}$, and $g$ = 2.21. The $1/\chi_M = f(\boldsymbol{T})$ curve (inset of figure 6) over the experimental temperature obeys the Curie–Weiss law with $C$ = 0.90 emu K M$^{-1}$ and $\theta$ = 3.01 K. The positive $J$ value and the Weiss constant indicate intramolecular ferromagnetic coupling between the unpaired electrons of Ru(III) centers of each dinuclear molecule, and the negative $zJ'$ value indicates intermolecular antiferromagnetism.

### 3.6. *DNA-binding studies*

The binding interaction of ruthenium complexes with DNA is increasingly studied; intercalation of complexes into the base pairs of DNA usually results in hypochromism (a decrease in the molar absorption coefficient) and bathochromism (red-shift). The binding ability of the complexes to CT-DNA was studied using electronic absorption spectroscopy, effective to examine the binding modes of metal complexes with DNA [20, 21]. The absorption spectral traces of the complexes with increasing concentration of CT-DNA are shown in figure 5. Upon addition of CT-DNA to **1** and **2**, hypochromism with bathochromism is observed, indicating a strong intercalation between the complexes and DNA base pairs (hypochromism, 43 and 30% for **1** and **2**, respectively) [22, 23]. A similar hyperchromism also has been observed for reported Ru(III)–EDTA complexes, where it was proposed that binding of DNA with Ru(III)–EDTA complexes takes place through the adenine base [24].

To further clarify the interaction of the complex with DNA, competitive binding using ethidium bromide (EB) as a probe was carried out. The fluorescence quenching of EB bound to CT-DNA by **1** and **2** is shown in figure 6. The addition of **1** or **2** to EB-bound CT-DNA solution caused obvious reduction in emission intensities, indicating complex

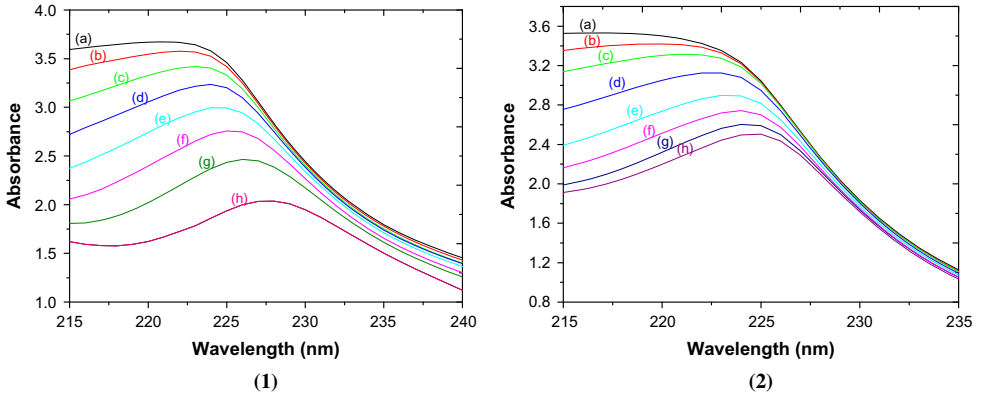


Figure 5. The UV–vis spectrum of **1** and **2**: (a) in the absence of DNA; (b) complex + DNA (2 μl); (c) complex + DNA (7 μl); (d) complex + DNA (12 μl); (e) complex + DNA (17 μl); (f) complex + DNA (22 μl); (g) complex + DNA (27 μl); (h) complex + DNA (32 μl).

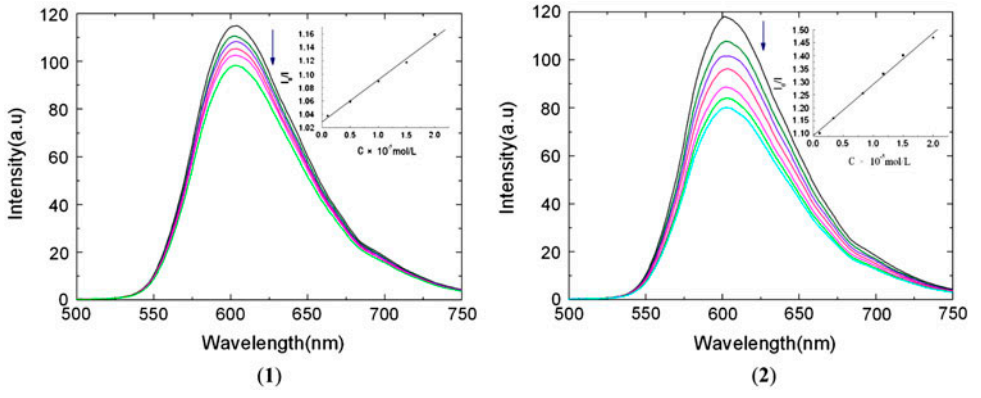


Figure 6. Fluorescence quenching of **1** and **2** to the EB-DNA system at room temperature. Inset: the plot of $I_0/I$ *vs.* $C$ ($I_0$ is the emission intensity EB-DNA in the absence of complexes, $I$ is emission intensity of EB-DNA in the presence of complexes, $C$ is the concentration of complexes).

competitively bound to CT-DNA with EB. The quenching plots illustrate that quenching of EB bound to DNA by the complexes are in agreement with the linear Stern–Volmer equation, which also indicates the complexes bind to DNA, in agreement with the change in electronic absorption data [25].

## 4. Conclusion

We report the synthesis of two new diruthenium(III) complexes, $[\{Ru(Hedta)\}_2(bpy)]\cdot 2H_2O$ (**1**) and $[\{Ru(Hedta)\}_2(Azpy)]\cdot 12H_2O$ (**2**). Magnetic studies show ferromagnetic interactions exist between the two ruthenium (III) ions in **1**, and the DNA-binding studies show that these complexes bind to CT-DNA through intercalation, which is of significance in regard to the assessment of DNA-targeting metallodrugs.

## Supplementary material

CCDC 286268 contains the supplementary crystallographic data for this paper. These data can be obtained free of charge at www.ccdc.cam.ac.uk/conts/retrieving.html [or from the Cambridge Crystallographic Data Center, 12 Union Road, Cambridge CB2 1EZ, UK; Fax: (internat.) + 44-1223-336-033; E-mail: deposit@ccdc.cam.ac.uk].

## Funding

This work was supported by the National Science Foundation of China [grant number 21101068]; the National Science Foundation of Anhui [grant number 1308085MB16]; and the Weifang Science and Technology Development Plan Project [grant number 201002057].

## References

[1] S.Q. Zhang, F.L. Jiang, M.Y. Wu, J. Ma, Y. Bu, M.C. Hong. *Cryst. Growth Des.*, **12**, 1452 (2012).
[2] M. Wriedt, H.C. "Joe" Zhou. *J. Chem. Soc., Dalton Trans.*, 4207 (2012).

[3] D. Chatterjee, A. Mitra, A. Levina, P.A. Lay. *Chem. Commun.*, **44**, 2864 (2008).
[4] D. Chatterjee, A. Mitra, M.S.A. Hamza, R.v. Eldik. *J. Chem. Soc., Dalton Trans.*, 962 (2002).
[5] M.R. Gill, J.A. Thomas. *Chem. Soc. Rev.*, **41**, 3179 (2012).
[6] I. Łakomska, M. Fandzloch, T. Muzioł, T. Lis, J. Jezierska. *J. Chem. Soc., Dalton Trans.*, 6219 (2013).
[7] H. Paul, T. Mukherjee, M.G.B. Drew, P. Chattopadhyay. *J. Coord. Chem.*, **65**, 1289 (2012).
[8] S. Sathiyaraj, R.J. Butcher, C. Jayabalakrishnan. *J. Coord. Chem.*, **66**, 580 (2013).
[9] J. Comiskey, E. Farkas, K.A. Krot-Lacina. *J. Chem. Soc., Dalton Trans.*, 4243 (2003).
[10] J.Y. Wang, W. Gu, W.Z. Wang, X. Liu, D.Z. Liao. *J. Coord. Chem.*, **64**, 2321 (2011).
[11] P. Day, C.K. Jorgensen. *Chem. Phys. Lett.*, **1**, 507 (1968).
[12] K. Natarajan, R.K. Poddar. *J. Inorg. Nucl. Chem.*, **39**, 431 (1977).
[13] J.Y. Wang, P.P. Yang, W. Gu, W.Z. Wang, X. Liu, D.Z. Liao. *J. Coord. Chem.*, **62**, 923 (2009).
[14] A.P.B. Lever. *Inorganic Electronic Spectroscopy*, 2nd Edn, Elsevier, New York (1989).
[15] O.K. Medhi, U. Agarwala. *Inorg. Chem.*, **19**, 1381 (1980).
[16] G. Giuffrida, G. Calorgero. *Inorg. Chem.*, **32**, 1179 (1993).
[17] Y. Wang, W.J. Perez, G.Y. Zheng. *Inorg. Chem.*, **37**, 2227 (1998).
[18] T.R. Weaver, T.J. Meyer, S.A. Adeyemi, G.M. Brown, R.P. Eckberg, W.E. Hatfield, E.C. Johnson, R.W. Murray, D. Untereker. *J. Am. Chem. Soc.*, **97**, 3039 (1975).
[19] M.A.S. Aquino, F.L. Lee, E.J. Gabe, J.E. Greedan, R.J. Crutchley. *Inorg. Chem.*, **30**, 3234 (1991).
[20] J.Z. Lu, Y.F. Du, H.W. Guo. *J. Coord. Chem.*, **64**, 1229 (2011).
[21] B.E. Smith, T.D. Lash. *Tetrahedron*, **66**, 4413 (2010).
[22] S.A. Tysoe, A.D. Baker, T.C. Strekas. *J. Phys. Chem.*, **97**, 1707 (1993).
[23] E.C. Long, J.K. Barton. *Acc. Chem. Res.*, **23**, 271 (1990).
[24] D. Chatterjee. *P. Indian As-Chem. Sci.*, **111**, 437 (1999).
[25] I. Ali, K. Saleem, D. Wesselinova, A. Haque. *Med. Chem. Res.*, **22**, 1386 (2013).